Water Resources Research

RESEARCH ARTICLE
10.1029/2018WR023609

Key Points:
- Reliable methods to predict permeability of naturally structured soils are currently lacking
- A percolation-based method applied to X-ray scanning data explained 47% of the variation in the measured permeability of 95 soil samples
- Variation in permeability was controlled by the critical pore diameter: the estimated effective porosity did not contribute significantly

Supporting Information:
- Supporting Information S1
- Data Set S1

Correspondence to:
J. Koestel,
john.koestel@slu.se

Citation:
Koestel, J., Dathe, A., Skaggs, T. H., Klakegg, O., Ahmad, M. A., Babko, M., et al. (2018). Estimating the permeability of naturally structured soil from percolation theory and pore space characteristics imaged by X-ray. *Water Resources Research*, *54*. https://doi.org/10.1029/2018WR023609

Received 3 JUL 2018
Accepted 23 OCT 2018
Accepted article online 30 OCT 2018

Estimating the Permeability of Naturally Structured Soil From Percolation Theory and Pore Space Characteristics Imaged by X-Ray

John Koestel[1], Annette Dathe[2], Todd H. Skaggs[3], Ove Klakegg[2], Muhammad Arslan Ahmad[1], Maryia Babko[1], Daniel Giménez[4], Csilla Farkas[2], Attila Nemes[2], and Nicholas Jarvis[1]

[1]Department of Soil and Environment, Swedish University of Agricultural Sciences, Uppsala, Sweden, [2]Norwegian Institute for Bioeconomy Research, Ås, Norway, [3]USDA-ARS Salinity Laboratory, Riverside, CA, USA, [4]Department of Environmental Sciences, Rutgers University, New Brunswick, NJ, USA

Abstract The saturated hydraulic conductivity of soil, K_s, is a critical parameter in hydrological models that remains notoriously difficult to predict. In this study, we test the capability of a model based on percolation theory and critical path analysis to estimate K_s measured on 95 undisturbed soil cores collected from contrasting soil types. One parameter (the pore geometry factor) was derived by model fitting, while the remaining two parameters (the critical pore diameter, d_c, and the effective porosity) were derived from X-ray computed tomography measurements. The model gave a highly significant fit to the K_s measurements ($p < 0.0001$) although only ~47% of the variation was explained and the fitted pore geometry factor was approximately 1 to 2 orders of magnitude larger than various theoretical values obtained for idealized porous media and pore network models. Apart from assumptions in the model that might not hold in reality, this could also be attributed to experimental error induced by, for example, air entrapment and changes in the soil pore structure occurring during sample presaturation and the measurement of K_s. Variation in the critical pore diameter, d_c, was the dominant source of variation in K_s, which suggests that d_c is a suitable length scale for predicting soil permeability. Thus, from the point of view of pedotransfer functions, it could be worthwhile to direct future research toward exploring the correlations of d_c with basic soil properties and site attributes.

1. Introduction

The saturated hydraulic conductivity of soil, K_s, is a key parameter determining the water balance of the land surface. Soil hydraulic conductivity can be measured on small cylinder samples in the laboratory (Klute & Dirksen, 1986) or with a variety of different infiltrometer techniques in the field (Angulo-Jaramillo et al., 2000). These methods are labor- and time-consuming and so they are not practical to apply in larger scale studies, for example, to support catchment-, regional-, and global-scale hydrological modeling. Since the 1990s, statistical techniques such as multivariate regression or machine learning techniques have therefore been employed to derive so-called pedotransfer functions that enable estimation of soil hydraulic properties from more easily available proxy variables (Bouma, 1989; Schaap et al., 2001; Wösten et al., 2001). A reasonably strong correlation is often found between soil water retention and the particle size distribution (Vereecken et al., 2010). In contrast, existing pedotransfer approaches for saturated hydraulic conductivity perform less well (e.g., Jarvis et al., 2013; Jorda et al., 2015; Vereecken et al., 2010). This is because K_s is largely governed by the properties of structural pores, which are only poorly correlated with the solid-phase properties (e.g., texture and organic carbon content) commonly used as predictors. In a modeling context, the use of inaccurate estimates of K_s may propagate into significant errors in predictions of water balance components such as runoff, infiltration, water storage, and evaporation (e.g., Chirico et al., 2010; Davis et al., 1999).

The application of noninvasive X-ray tomography (Helliwell et al., 2013) may help to improve our understanding of how K_s is controlled by the geometry and topology of structural pore networks. Some local-scale studies have found significant statistical relationships between various X-ray imaged metrics of the pore space and K_s measured on the same samples (e.g., Kim et al., 2010; Luo et al., 2010; Udawatta et al., 2008). However, physics-based models of K_s should allow deeper insight into how the properties of soil pore networks control K_s and, arguably, more reliable extrapolation beyond the constraints of the supporting data. Many models have been proposed to predict K_s from characteristics of the soil pore space (Assouline & Or, 2013). Most

Table 1
Field Sites for Sampling

Profile number	Land use	Number of cores	Texture	Horizons sampled	Taxonomy
101942	Grains/potato	4	silt loam/silt loam	A_p, B_w	Dystric Fluvic Endostagnic Cambisol
101945	Grains/potato	4	silt/silt loam	A_p, B_g	Dystric Fluvic Mollic Stagnosol
101972	Grains	2	Loam	A_p	Cambic Chernic Phaeozem
101973	Grass	2	Loam	A_p	Chernic Phaeozem
101946	Grains	1	Loam	A_p	Haplic Phaeozem
101947	Grains	4	silt loam/silt loam	A_p, B_w	Stagnic Cambisol
101948	Grains	4	clay loam/silty clay loam	A_p, B_g	Mollic Planosol
101949	Grains	2	sandy loam	A_p	Eutric Stagnic Cambisol
101950	Grains	2	Loam	A_p	Stagnic Phaeozem
101951	Grains	4	silt loam/silt loam	A_p, C_g	Mollic Gleysol
101952	Grass	4	sandy loam/loam	A_p, B_g	Fluvic Umbric Gleysol
101954	Grains	4	loam/loam	A_p, B_w	Haplic Phaeozem
101955	Grains	3	sandy loam	A_p	Mollic Stagnosol
101967	Grass	2	silt	C	Eutric Protic Regosol
101969	Grass	4	sandy loam/silt loam	$A_{p(g)}$, C	Dystric Fluvic Gleysol
Skuterud	Grains	43	silty clay loam	A_p, B_g, B_{tg}	Luvic Stagnosol

approaches derive from the Kozeny-Carman model first developed nearly 100 years ago, which assumes that flow rates are controlled by a single *effective* pore. As such, in its original form it can successfully describe K_s for porous media characterized by a relatively well-connected pore space and uniform-sized pores. However, it will fail in natural soils characterized by a wide distribution of pore sizes, since water flow at saturation is dominated by a few large, continuous, pores (Childs, 1969).

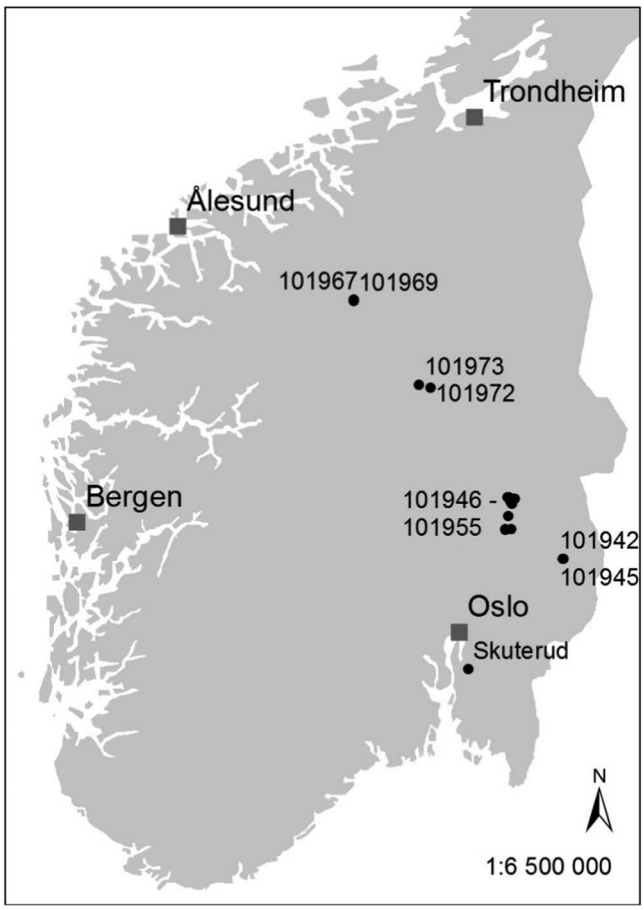

Figure 1. Map of the sampling locations in Norway.

The Kozeny-Carman equation has been generalized in an attempt to explicitly account for the effects of soil pore size distribution using the soil water retention function as a proxy and making use of the Young-Laplace equation to relate pore size to soil water tension. These capillary bundle models are widely used to estimate unsaturated hydraulic conductivity from an independently measured K_s value and knowledge of the water retention characteristic (Assouline & Or, 2013). Although it is less often done, they can also be used to estimate K_s (e.g., Jarvis, 2008; Laliberte et al., 1968; Mishra & Parker, 1990; Nasta et al., 2013). The few studies that have tested capillary bundle models against measured data show that K_s is strongly overestimated for most, but not necessarily all, soils for physically realistic values of the pore tortuosity factor (e.g., Hoffmann-Riem et al., 1999; Jarvis, 2008; Nasta et al., 2013). This is probably because the conceptual basis of capillary bundle models (i.e., noninteracting parallel or series-parallel pores) cannot properly account for the significant effects of pore connectivity on K_s (Hunt et al., 2013).

In contrast with generalized Kozeny-Carman type models, approaches based on critical path analysis (CPA) and percolation theory may prove to be better suited to predict K_s in naturally structured soils. Percolation-based models of conducting porous media envisage that flow takes place through a *percolating* network of pores consisting of multiple connected pathways (Hunt et al., 2014). CPA is based on the premise that flow through a pore network characterized by a very wide range of conductances is limited by the smallest (i.e., *bottleneck*) pore thickness on the path of least resistance through the sample. Percolation and CPA-based approaches have been successfully applied to predict the permeability of rocks and artificial porous materials such as ceramics and concrete (Arns et al., 2005; Ghanbarian et al., 2016; Katz & Thompson, 1986; Nishiyama & Yokoyama, 2014, 2017; Nokken & Hooton, 2008), but they have not yet been critically tested on soils. A

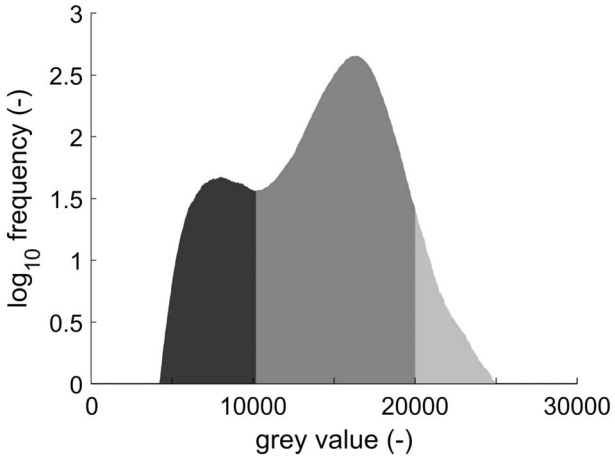

Figure 2. Joint histogram of the gray values of the 95 3-D images. The parts of the histogram shown in dark gray correspond to air-filled pores as defined by a joint threshold value of 10,171 obtained using the minimum method. Voxels with X-ray attenuation values larger than that of aluminum (grayscale values larger than 20,000) are depicted in a lighter gray. The remaining grayscale values predominantly correspond to the soil matrix (e.g., solid matter and water-filled pores smaller than image resolution).

recent study by Ghanbarian et al. (2017) compared K_s estimates derived from a fractal CPA model with average measured values for U.S. Department of Agriculture soil texture classes, but this model was not tested against data for individual soil samples. Furthermore, the model parameters were estimated indirectly. In particular, the percolation threshold was equated with the residual water content determined from water retention curves, a procedure which may provide values of the right order of magnitude, but which lacks physical justification. Here we tested the capability of a percolation/CPA-based model to predict K_s of 95 soil cores collected in Norway from a wide range of contrasting soil types under differing land uses (arable land and grassland) with the model parameters derived directly from high-resolution X-ray scanning.

2. Materials and Method

2.1. Theory

Using concepts from percolation theory and CPA, Katz and Thompson (1986) derived an expression for the saturated hydraulic conductivity of a percolating porous medium characterized by a very wide distribution of local hydraulic conductances:

$$K_s = \left(\frac{1}{G}\right)\sigma_r d_c^2\left(\frac{\rho\, g}{\eta}\right) \tag{1}$$

where g is the acceleration due to gravity (L/T^2); η ($M \cdot L^{-1} \cdot T^{-1}$) and ρ (M/L^3) are the dynamic viscosity and density of water; d_c is the *critical* pore diameter (L), defined as the smallest pore neck encountered along the path of least resistance through the sample; σ_r (−) is the reciprocal of the electrical conductivity *formation factor* (i.e., the bulk soil electrical conductivity divided by the conductivity of the saturating fluid); and G (−) is a geometry factor, the value of which varies depending on assumptions concerning pore shape (i.e., cylinders or slits) and aspect ratio (i.e., the relationship between pore length and diameter) as well as the width of the conductance distribution (Skaggs, 2011). From theoretical considerations, values for G as small as 27 (for slits of equal length and variable diameter) and as large as 85, 130, or 226 (for cylinders of equal length and diameter) have been suggested (e.g., Banavar & Johnson, 1987; Katz & Thompson, 1986; Le Doussal, 1989; Skaggs, 2003, 2011).

The relative electrical conductivity term in equation (1) represents an effective (conducting) porosity in soil, ϕ_{eff}, accounting for the connectivity of the pore space. In the absence of direct measurements of electrical conductivity, Katz and Thompson (1987) showed that ϕ_{eff} could be defined as

$$\sigma_r = \phi_{\text{eff}} = \phi_p\left[\frac{d_{\text{opt}}}{d_c}\right] \tag{2}$$

where ϕ_p is the accessible percolating porosity with thicknesses larger than d_{opt}, a value corresponding to the optimal path for electrical conductance. Katz and Thompson (1987) also proposed a method to estimate d_{opt} for individual samples from the accessible pore size distribution obtained from mercury intrusion experiments. In our study, we adopted a simpler approach to estimate d_{opt} based on the assumption that for wide distributions of pore thickness, d_{opt} can be estimated from $[1 - (t/(1+t))]d_c$ where t is a critical exponent from percolation theory, which equals 2 in three dimensions (Ghanbarian et al., 2017; Katz & Thompson, 1987; Stauffer & Aharony, 1994). Thus, in this study, ϕ_{eff} is given by one third of ϕ_p, where ϕ_p is the accessible and percolating porosity corresponding to pores thicker than $d_c/3$.

2.2. Sampling and Experimental Measurements

Aluminum cylinders (6.5 cm in inner diameter and 6 cm in height) were used to collect all the samples used in this study. Forty-three samples were from the Skuterud catchment situated approximately 30 km south of Oslo and 2.5 km east of Ås (Table 1 and Figure 1). These cores were collected as part of an ongoing field experiment from two soil pits spaced 5 m apart, at soil depths from 10 to 90 cm. A further 46 undisturbed

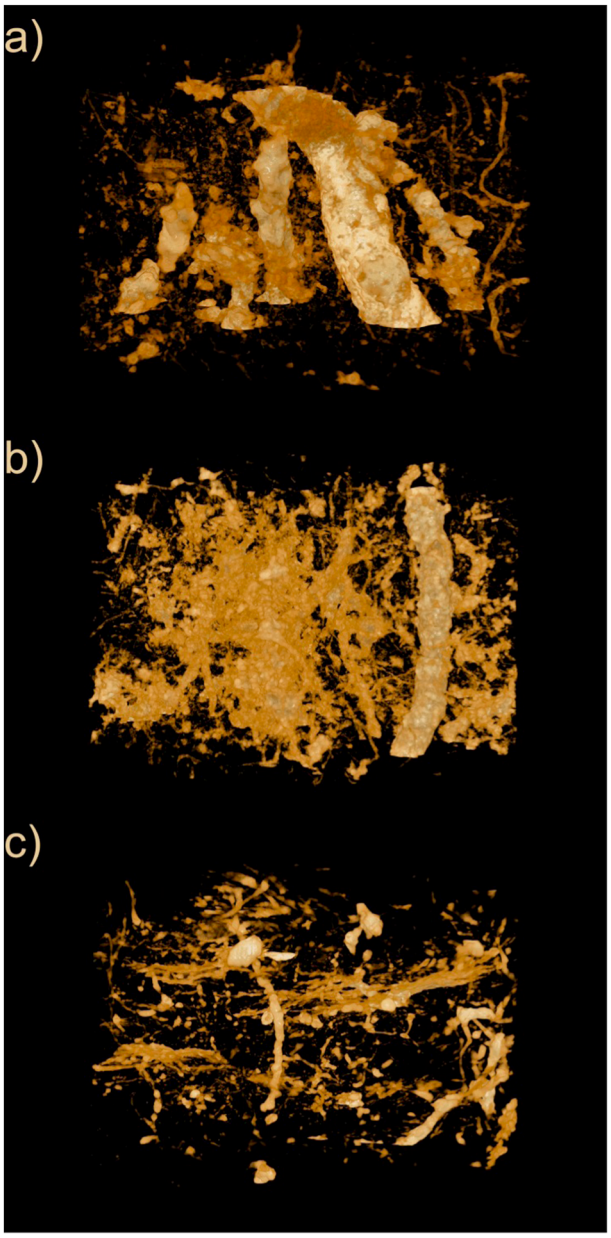

Figure 3. X-ray images of the cores with (a) the largest critical pore diameter (A_p horizon at site 101952; d_c = 1.85 mm), (b.) the largest K_s value (=257 cm/hr; topsoil sample from Skuterud), and (c) the smallest K_s value at Skuterud (=0.004 cm/h).

soil cores were sampled at 15 additional sites across Norway from topsoil and subsoil horizons (Table 1 and Figure 1). To complement and contrast with the data from these structured and mostly fine-textured soils, we also included data for six cores that were sampled from a vermi-compost experiment carried out in Ås, Norway, in which a sandy soil originating from Nyírség in Hungary was mixed with different organic amendments (at 2% by weight).

The cores were stored in a cold room at 3 °C. We then equilibrated them at a pressure head of −100 cm on a sand table for approximately 1 week to ensure that all pores quantifiable by X-ray tomography would be air-filled. They were then scanned using a GE v|tome|x 240 X-ray scanner with a tungsten target and a 16″ flat panel detector. We applied tube voltages between 150 and 170 kV and electron fluxes between 300 and 600 μA, depending on the density of the soil column. We did not apply an optical filter to the X-ray beam. The image resolution was 0.04 mm in all directions for all columns, which corresponds to a feature resolution of approximately 0.08 mm. After X-ray scanning, the saturated hydraulic conductivity of each core was measured using a constant head method in the laboratory after slowly saturating the samples from the base during a two-week period. The smallest K_s value that can be measured by this method, in practice, is approximately 0.05 mm/hr (= ~1.4×10^{-8} m/s).

We processed the X-ray images using SoilJ (Koestel, 2018), a plugin for the free software ImageJ/FIJI (Schindelin et al., 2012) that allows for a semiautomatized image processing and analyses of 3-D images of cylindrical soil columns. In the first processing steps, the soil column outlines were automatically detected and the column was moved into the center of the image canvas. Unused canvas was cut away as well as image slides depicting the air and the Styrofoam above and below the soil column, respectively. Next, we calibrated the gray scale of all 95 16-bit images to values of 5,000 for air and 20,000 for aluminum. The calibration was carried out layer-by-layer where the 0.1 percentile of the grayscale value sampled inside the soil column was employed as the reference value for air, while the value for the column wall was used as the reference for aluminum. Subsequently, we calculated the joint histogram for all 95 calibrated 3-D images (see Figure 2) and a joint-threshold grayscale value of 10,171 was determined by the minimum method (Tsai, 1995). As was also done by Hellner et al. (2018), we applied this threshold value to all gray-scale-calibrated images to obtain binary images depicting the X-ray resolvable pores. Beckers et al. (2014) found that a similar global segmentation method performed as well as local approaches that are more demanding in terms of time and computational resources. Figures 3a–3c depict three example images of samples showing contrasting pore space structure.

We identified individual percolating pore clusters in the binary images using the parallelized *Particle Analyzer* algorithm published under the BoneJ plugin (Doube et al., 2010). The critical pore diameter d_c, which can be defined as the diameter of the largest sphere that passes through the pore network (e.g., Arns et al., 2005), was then calculated in SoilJ. Local pore diameters of the percolating pore space were determined using the maximal inscribed ball method implemented in ImageJ (*Local Thickness*). The effective porosity ϕ_{eff} was then calculated using equation (2) from d_c and the percolating and accessible pore space (i.e., connected from top to bottom of the core only by pore space of thickness larger than $d_c/3$; see Figure 4; Katz & Thompson, 1987). It should be noted that the image resolution (0.04 mm) has some influence on the results. For example, one of the 95 samples had no visible percolating porosity. For plotting purposes only, the critical pore diameter for this sample was set to the image resolution and the effective porosity to a nominal value of

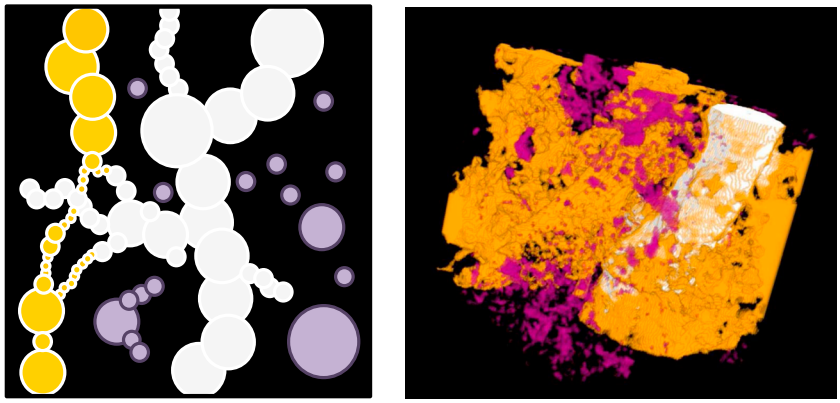

Figure 4. Illustration of the method used to estimate the effective porosity from X-ray images. The schematic figure to the left shows the effective porosity in light grey. This pore space is thicker than one third of the critical pore diameter d_c and is also both accessible and connected to a percolating cluster. The yellow-colored pore space is part of the percolating cluster, and some is also thicker than $d_c/3$. However, these pores are not accessible because they are only connected through pore necks smaller than $d_c/3$. The lilac-colored pore space is disconnected (i.e., not percolating at the image resolution). The figure to the right shows an actual X-ray image with the pore space classified and colored in the same way.

0.1%. In addition, measured d_c values were smaller than 0.12 mm (i.e., 3 times the image resolution) for seven columns, which suggests that ϕ_{eff} would be underestimated for these samples, since the estimated value of d_{opt} was smaller than the image resolution.

The complex and highly variable geometry of soil structural pore networks suggests that G in equation (1) should be treated as a fitting parameter. We estimated G from ordinary linear regression without intercept using the experimentally measured K_s values, the values of d_c and ϕ_{eff} obtained from the X-ray analysis, and known values of ρ, g, and η at 20 °C. The square of the correlation coefficient between the estimated and measured values of log (K_s) was taken as a measure of the proportion of variance explained by the model, since linear regression without an intercept gives artificially inflated estimates of R^2.

3. Results and Discussion

Figures 5a–5c show the distributions of the critical pore diameter, d_c; the estimated effective porosity, ϕ_{eff}; and the measured K_s values for the 95 samples. The critical pore diameter appeared to be lognormally distributed, with a median d_c value of 0.33 mm and an interquartile range of 0.35 mm (0.16–0.55 mm; Figure 5a). Thus, although many d_c values were relatively small, lying close to the feature resolution (0.08 mm), nearly 30% of the samples had critical pore diameters larger than 0.5 mm, which indicate the presence of one or more structural macropores connected across the sample (see the examples in Figures 3a–3c) that may dramatically increase K_s values (e.g., Jarvis et al., 2013; Jorda et al., 2015). The median value of the effective porosity was 3.2%, with an interquartile range of 1.4 to 7.2% (Figure 5b). The effective porosity and the critical pore diameter were not significantly correlated (Figure 6; $p = 0.62$). The median value of the saturated hydraulic conductivity was 3.84 cm/h, but as is commonly found, the K_s values varied widely, ranging across approximately 6 orders of magnitude, with lower and upper quartile values of 0.36 and 26 cm/h (Figure 5c) and a coefficient of variation of 215%.

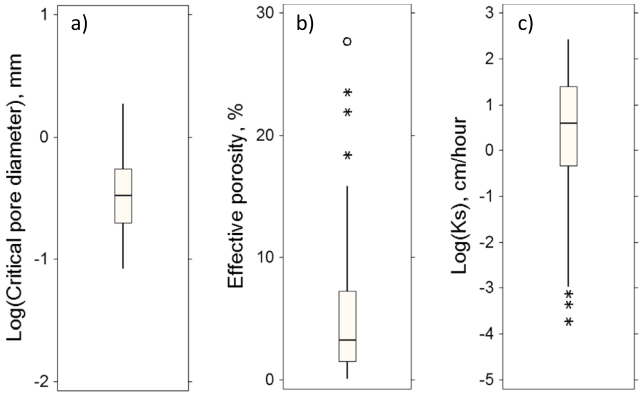

Figure 5. The box and whisker plots of critical pore diameter (d_c), effective porosity (ϕ_{eff}), and saturated hydraulic conductivity (K_s). The horizontal lines indicate medians, the length of the box shows the inter-quartile range, and the whiskers indicate the range of typical values. Possible and probable outliers indicated by asterisks and open symbols are defined as values that lie outside the box boundaries by more than 1.5 and 3 times the size of the box respectively.

The fit obtained with the Katz and Thompson model described by equations (1) and (2) was significant at $p < 0.0001$, with a best fit value of G of 3162 (Figures 7 and 8) and no apparent bias in the estimates across approximately 4 orders of magnitude, except at very small measured K_s values (< 0.01 cm/hr). Nevertheless, Figure 8 shows that there is considerable scatter in the relationship between estimated and measured K_s

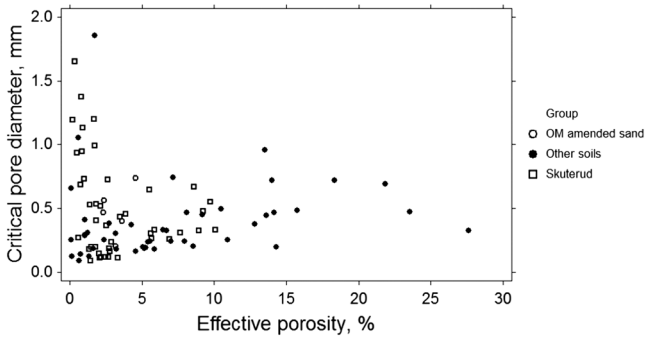

Figure 6. The relationship between critical pore diameter, d_c, and effective porosity, ϕ_{eff}.

values. Only 47% of the variation in log (K_s) was explained by the model, and the predictions were in error by more than 1 order of magnitude for approximately 30% of the data points. The fitted value of G is approximately 1 to 2 orders of magnitude larger than theoretical values (27 to 226, see above) previously derived for idealized porous media and pore network models and also lies outside the range (approximately 333 to 1820) found experimentally by Nishiyama and Yokoyama (2017) for a wide range of different porous rocks and artificial (man-made) porous media (e.g., cement, concrete). Furthermore, in contrast to our results, Nishiyama and Yokoyama (2017) showed that the Katz and Thompson model accurately estimated permeability ($R^2 > 0.96$). Errors and uncertainties in the measurements may have contributed significantly to the much poorer predictions of K_s and the larger estimate of G for our naturally structured soils. For example, after X-ray scanning, the pore space structure of many of our samples may have changed during presaturation prior to K_s measurement or during the measurement of K_s, either due to the swelling of clay minerals, the consolidation of structurally unstable soils, or the activity of macrofauna (e.g., earthworms). This is illustrated for one core sample in Figure 9. These images were taken before and after presaturation and K_s measurement and show evidence of both pore space consolidation and shrinkage crack formation. One potential solution to this problem would be to make measurements on printed copies of X-ray imaged samples, although some technical issues remain to be resolved (Bacher et al., 2015).

Air entrapment has also been shown to occur in structural pores during sample presaturation and infiltration (Koestel & Larsbo, 2014; Luo et al., 2008; Luo & Lin, 2009; Sněhota et al., 2010). Babko (2016) measured entrapped air contents after presaturation for five of the samples from the Skuterud field site in Norway with imaged porosities between 3 and 7%. This experiment showed that between 25 and 65% of the imaged porosity contained trapped air, with larger values found for the samples of smaller imaged porosity. Following vacuum saturation, trapped air contents were subsequently reduced to close to 0, while K_s more than doubled in one sample and increased by approximately 10% in two others. However, K_s was only marginally affected in the two remaining samples (Babko, 2016). As also found by Jarvis et al. (2017) and predicted by percolation theory, the connectivity of the structural pore space in our data set decreases significantly as the imaged porosity decreases toward a threshold value for long-range continuity (or percolation; Figure 10). Furthermore, during saturation entrapped air will tend to collect in the larger pores (Sněhota et al., 2010). All this suggests that air entrapment could have a disproportionally large effect on the permeability of soils with small structural porosity. Thus, it seems probable that the comparatively large estimated value of G and the large systematic overestimation of permeability for samples with measured K_s values less than approximately 0.1 cm/hr (Figures 7 and 8) are at least partly a consequence of air entrapment. Although air can be removed from samples by vacuum saturation with degassed water, such conditions would rarely occur in the field. Such an experimental approach would also make it difficult to compare K_s values with data obtained in previous studies, where air entrapment has been tacitly accepted.

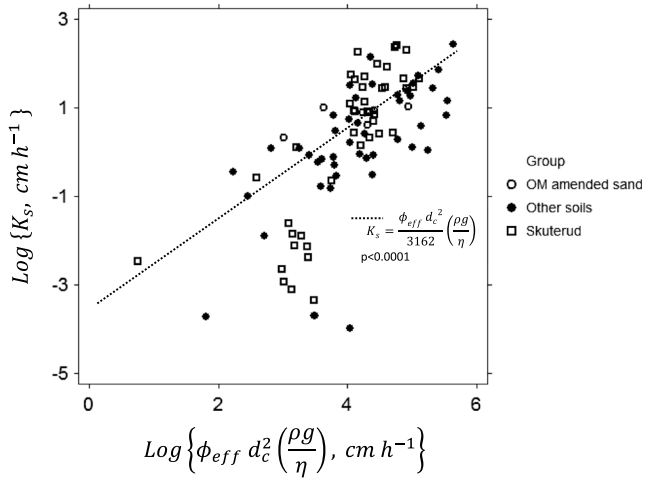

Figure 7. Measured saturated hydraulic conductivity, K_s, as a function of ϕ_{eff} d_c^2. The dotted line shows the best fit from ordinary linear regression without intercept (slope = 1/3162).

A simple empirical model based solely on d_c and not ϕ_{eff} (equation (3) with a fitted value of G of 68074; $p < 0.0001$) explained almost as much (45%) of the variation in log (K_s) as the full model given by equation (1), in combination with equation (2):

$$K_s = \frac{d_c^2}{G}\left(\frac{\rho\, g}{\eta}\right) \tag{3}$$

This suggests that although the critical pore diameter appears to be a good length scale for predicting soil permeability, the effective porosity (the reciprocal of the formation factor) may have been poorly estimated

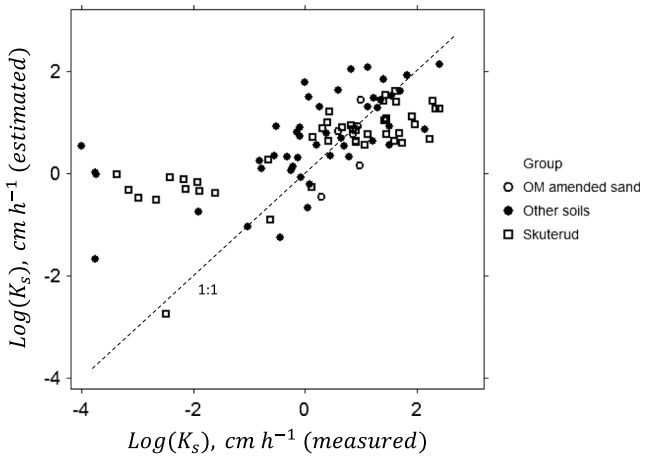

Figure 8. Measured K_s and estimated values using equations (1) and (2) with G = 3162.

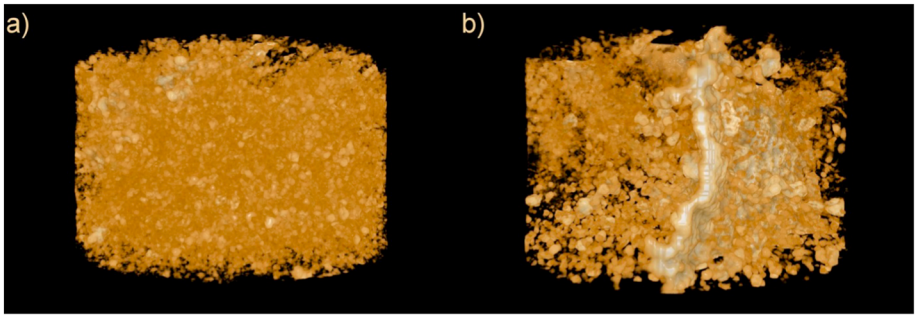

Figure 9. X-ray images of the pore space of a sample taken from the silt A_p horizon at site 101945, (a) before and (b) after sample presaturation and measurement of K_s.

by the simple method employed in this study. Another likely reason for the poor performance of the CPA-percolation model is that one or more of the key assumptions underlying its derivation were not sufficiently valid. CPA-theory relies on the assumption that the distribution of local (pore-scale) conductances is broad and that they are not spatially correlated. Under these conditions flow at saturation should be dominated by the *bottleneck* resistance along the critical path. The first assumption may be reasonable for many naturally structured soils, although some of our samples may not have met this requirement (e.g., the packed sands amended by organic matter and the natural sandy loam soils; Table 1). With regard to the second assumption, it seems highly probable that for the size of our samples, the structural pore space imaged by X-ray cannot be adequately described as the outcome of a spatially

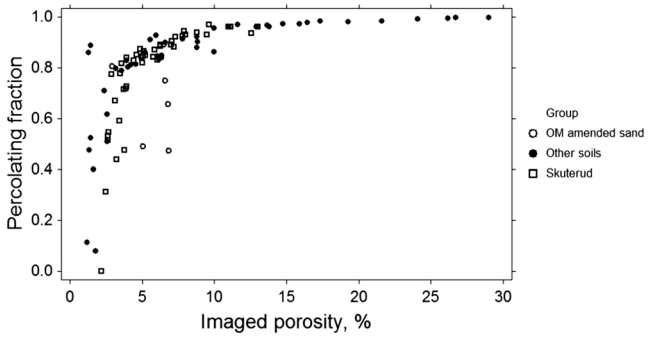

Figure 10. The percolating fraction of the imaged porosity as a function of imaged porosity.

uncorrelated (random) arrangement of pore space (see the examples in Figures 3a–3d; Jarvis et al., 2017). If these assumptions are not met, flow may be less localized than is envisioned in classical CPA (e.g., Bernabé & Bruderer, 1998; Friedman & Seaton, 1998; Skaggs, 2003, 2011) and theoretical predictions of the relative electrical conductivity (effective porosity) and the coefficient G will be less reliable.

4. Conclusions

The critical pore diameter, d_c, appears to be a suitable length scale for predicting the saturated hydraulic conductivity of soil, K_s. Physical and semiempirical models based on d_c are also parsimonious and may therefore represent suitable approaches for estimating K_s in hydrological models, despite large prediction uncertainties. From this point of view, it could therefore be worthwhile to direct future research toward exploring the correlations of d_c with basic soil properties and site attributes. The effective porosity (or inverse of the formation factor) estimated by the simple approach employed here did not contribute significantly to explaining the variation in K_s. It may therefore be worthwhile testing whether the more advanced method suggested by Katz and Thompson (1987) to estimate effective porosity from measurements of the thickness distribution of the accessible pore space could give improved predictions of K_s. An inadequate sample size was thought to be another important reason for the large uncertainty in predictions of K_s using the percolation-based models. It could therefore also be valuable to make use of X-ray scanning techniques to revisit the long-standing issue of the size of sample needed to adequately capture the scale of the heterogeneity found in structured soils, focusing especially on the variations of the percolating pore space and the critical pore diameter with sample size, since these parameters will significantly affect water flow at and near saturation.

Data Statement

The authors have uploaded a copy of the data as supporting information.

Acknowledgments
This work was carried out in the project SOILSPACE ("Quantifying soil structure to augment the relevance of laboratory-based soil hydraulic properties for environmental modelling") funded by the Research Council of Norway (project 240663). We would like to thank Eivind Solbakken and Åge Nyborg (both at NIBIO) for assistance with the field sampling, together with students Julia Szocs, Erin Ball, Jonas Reinemo, Matthew Patterson, and Mingming Qin. We would also like to thank Claudia von Brömssen (Department of Energy and Technology, Unit of Applied Statistics and Mathematics, SLU) for helpful advice on statistics.

References

Angulo-Jaramillo, R., Vandervaere, J.-P., Roulier, S., Thony, J.-L., Gaudet, J.-P., & Vauclin, M. (2000). Field measurement of soil surface hydraulic properties. A review and recent developments. *Soil and Tillage Research*, *55*(1–29), 2000.

Arns, C. H., Knackstedt, M. A., & Martys, N. S. (2005). Cross-property correlations and permeability estimation in sandstone. *Physical Review E*, *72*(4), 046304. https://doi.org/10.1103/PhysRevE.72.046304

Assouline, S., & Or, D. (2013). Conceptual and parametric representation of soil hydraulic properties: A review. *Vadose Zone Journal*, *12*(4). https://doi.org/10.2136/vzj2013.07.0121

Babko, M. (2016). What is the impact of entrapped air on the measurement of saturated hydraulic conductivity of soil? (Master's thesis, 28 pp.) Dept. Soil and Environment, Swedish University Agric. Sci., Uppsala, Sweden.

Bacher, M., Schwen, A., & Koestel, J. (2015). Three-dimensional printing of macropore networks of an undisturbed soil sample. *Vadose Zone Journal*, *14*(2). https://doi.org/10.2136/vzj2014.08.0111

Banavar, J. R., & Johnson, D. L. (1987). Characteristic pore sizes and transport in porous media. *Physical Review B*, *35*(13), 7283–7286. https://doi.org/10.1103/PhysRevB.35.7283

Beckers, E., Plougonven, E., Roisin, C., Hapca, S., Leonard, A., & Degre, A. (2014). X-ray microtomography: A porosity-based thresholding method to improve soil pore network characterization? *Geoderma*, *219-220*, 145–154. https://doi.org/10.1016/j.geoderma.2014.01.004

Bernabé, Y., & Bruderer, C. (1998). Effect of the variance of pore size distribution on the transport properties of heterogeneous networks. *Journal of Geophysical Research*, *103*(B1), 513–525. https://doi.org/10.1029/97JB02486

Bouma, J. (1989). Using soil survey data for quantitative land evaluation. *Advances in Soil Science*, *9*, 177–213. https://doi.org/10.1007/978-1-4612-3532-3_4

Childs, E. C. (1969). *An introduction to the physical basis of soil water phenomena*. London: John Wiley.

Chirico, G. B., Medina, H., & Romano, N. (2010). Functional evaluation of PTF prediction uncertainty: An application at hillslope scale. *Geoderma*, *155*(3-4), 193–202. https://doi.org/10.1016/j.geoderma.2009.06.008

Davis, S. H., Vertessy, R. A., & Silberstein, R. P. (1999). The sensitivity of a catchment model to soil hydraulic properties obtained by using different measurement techniques. *Hydrological Processes*, *13*(5), 677–688. https://doi.org/10.1002/(SICI)1099-1085(19990415)13:5<677::AID-HYP772>3.0.CO;2-N

Doube, M., Klosowski, M. M., Arganda-Carreras, I., Cordelieres, F. P., Dougherty, R. P., Jackson, J. S., et al. (2010). BoneJ free and extensible bone image analysis in Image. *J Bone*, *47*(6), 1076–1079. https://doi.org/10.1016/j.bone.2010.08.023

Friedman, S. P., & Seaton, N. A. (1998). Critical path analysis of the relationship between permeability and electrical conductivity of three-dimensional pore networks. *Water Resources Research*, *34*(7), 1703–1710. https://doi.org/10.1029/98WR00939

Ghanbarian, B., Hunt, A. G., Skaggs, T. H., & Jarvis, N. (2017). Upscaling soil saturated hydraulic conductivity from pore throat characteristics. *Advances in Water Resources*, *104*, 105–113. https://doi.org/10.1016/j.advwatres.2017.03.016

Ghanbarian, B., Torres-Verdin, C., & Skaggs, T. H. (2016). Quantifying tight-gas sandstone permeability via critical path analysis. *Advances in Water Resources*, *92*, 316–322. https://doi.org/10.1016/j.advwatres.2016.04.015

Helliwell, J. R., Sturrock, C. J., Grayling, K. M., Tracy, S. R., Flavel, R. J., Young, I. M., et al. (2013). Applications of X-ray computed tomography for examining biophysical interactions and structural development in soil systems: A review. *European Journal of Soil Science*, *64*(3), 279–297. https://doi.org/10.1111/ejss.12028

Hellner, Q., Koestel, J., Ulén, B., & Larsbo, M. (2018). Effects of tillage and liming on macropore networks derived from X-ray tomography images of a silty clay soil. *Soil Use and Management* https://doi.org/10.1111/sum.12418, *34*(2), 197–205.
Hoffmann-Riem, H., van Genuchten, M. T., & Flühler, H. (1999). General model of the hydraulic conductivity of unsaturated The Soil. In M. T. van Genuchten, F. J. Leij, & L. Wu (Eds.), *Characterization and Measurement of the hydraulic properties of unsaturated porous Media, Part 1* (pp. 31–42). Riverside, CA: USDA.
Hunt, A., Ewing, R., & Ghanbarian, B. (2014). *Percolation theory for flow in porous media*. *Lecture notes in physics 880*. Heidelberg, Germany: Springer-Verlag. https://doi.org/10.1007/978-3-319-03771-4
Hunt, A. G., Ewing, R. P., & Horton, R. (2013). What's wrong with soil physics? *Soil Science Society of America Journal*, *77*(6), 1877–1887. https://doi.org/10.2136/sssaj2013.01.0020
Jarvis, N., Koestel, J., Messing, I., Moeys, J., & Lindahl, A. (2013). Influence of soil, land use and climatic factors on the hydraulic conductivity of soil. *Hydrology and Earth System Sciences*, *17*(12), 5185–5195. https://doi.org/10.5194/hess-17-5185-2013
Jarvis, N. J. (2008). Near-saturated hydraulic properties of macroporous soils. *Vadose Zone Journal*, *7*, 1256–1264.
Jarvis, N. J., Larsbo, M., & Koestel, J. (2017). Connectivity and percolation of structural pore networks in a cultivated silt loam soil quantified by X-ray tomography. *Geoderma*, *287*, 71–79. https://doi.org/10.1016/j.geoderma.2016.06.026
Jorda, H., Bechtold, M., Jarvis, N., & Koestel, J. (2015). Using boosted regression trees to explore key factors controlling saturated and near-saturated hydraulic conductivity. *European Journal of Soil Science*, *66*(4), 744–756. https://doi.org/10.1111/ejss.12249
Katz, A. J., & Thompson, A. H. (1986). Quantitative prediction of permeability in porous rock. *Physical Review B*, *34*(11), 8179–8181. https://doi.org/10.1103/PhysRevB.34.8179
Katz, A. J., & Thompson, A. H. (1987). Prediction of rock electrical conductivity from mercury injection measurements. *Journal of Geophysical Research*, *92*(B1), 599–607. https://doi.org/10.1029/JB092iB01p00599
Kim, H., Anderson, S. H., Motavalli, P. P., & Gantzer, C. J. (2010). Compaction effects on soil macropore geometry and related parameters for an arable field. *Geoderma*, *160*(2), 244–251. https://doi.org/10.1016/j.geoderma.2010.09.030
Klute, A., & Dirksen, C. (1986). Hydraulic conductivity and diffusivity: laboratory methods. In A. Klute (Ed.), *Methods of soil analysis. Part 1—Physical and mineralogical methods* (pp. 687–734). Madison, WI: ASA/SSSAJ.
Koestel, J. (2018). SoilJ: An ImageJ plugin for the semiautomatic processing of three-dimensional X-ray images of soils. *Vadose Zone Journal*, 170062. https://doi.org/10.2136/vzj2017.03.0062
Koestel, J., & Larsbo, M. (2014). Imaging and quantification of preferential solute transport in soil macropores. *Water Resources Research*, *50*, 4357–4378. https://doi.org/10.1002/2014WR015351
Laliberte, G. E., Brooks, R. H., & Corey, A. T. (1968). Permeability calculated from desaturation data. *Journal of the Irrigation and Drainage Division, Proc. ASCE*, *94*, 57–71.
Le Doussal, P. (1989). Permeability versus conductivity for porous media with wide distribution of pore sizes. *Physical Review B*, *39*(7), 4816–4819. https://doi.org/10.1103/PhysRevB.39.4816
Luo, L., & Lin, H. (2009). Lacunarity and fractal analyses of soil macropores and preferential transport using micro-X-ray computed tomography. *Vadose Zone Journal*, *8*(1), 233–241. https://doi.org/10.2136/vzj2008.0010
Luo, L., Lin, H., & Halleck, P. (2008). Quantifying soil structure and preferential flow in intact soil using X-ray computed tomography. *Soil Science Society of America Journal*, *72*(4), 1058–1069. https://doi.org/10.2136/sssaj2007.0179
Luo, L., Lin, H., & Schmidt, J. (2010). Quantitative relationships between soil macropore characteristics and preferential flow and transport. *Soil Science Society of America Journal*, *74*(6), 1929–1937. https://doi.org/10.2136/sssaj2010.0062
Mishra, S., & Parker, J. C. (1990). On the relation between saturated conductivity and capillary retention characteristics. *Ground Water*, *28*(5), 775–777. https://doi.org/10.1111/j.1745-6584.1990.tb01991.x
Nasta, P., Vrugt, J. A., & Romano, N. (2013). Prediction of the saturated hydraulic conductivity from Brooks and Corey's water retention parameters. *Water Resources Research*, *49*, 2918–2925. https://doi.org/10.1002/wrcr.20269
Nishiyama, N., & Yokoyama, T. (2014). Estimation of permeability of sedimentary rocks by applying water-expulsion porosimetry to Katz and Thompson model. *Engineering Geology*, *177*, 75–82. https://doi.org/10.1016/j.enggeo.2014.05.016
Nishiyama, N., & Yokoyama, T. (2017). Permeability of porous media—Role of the critical pore size. *Journal of Geophysical Research: Solid Earth*, *122*, 6955–6971. https://doi.org/10.1002/2016JB013793
Nokken, M. R., & Hooton, R. D. (2008). Using pore parameters to estimate permeability or conductivity of concrete. *Materials and Structures*, *41*, 1–16.
Schaap, M. G., Leij, F. J., & van Genuchten, M. T. (2001). ROSETTA: A computer program for estimating soil hydraulic parameters with hierarchical pedotransfer functions. *Journal of Hydrology*, *251*(3-4), 163–176. https://doi.org/10.1016/S0022-1694(01)00466-8
Schindelin, J., Arganda-Carreras, I., Frise, E., Kaynig, V., Longair, M., Pietzsch, T., et al. (2012). Fiji: An open-source platform for biological-image analysis. *Nature Methods*, *9*(7), 676–682. https://doi.org/10.1038/nmeth.2019
Skaggs, T. H. (2003). Effects of finite system size and finite inhomogeneity on the conductivity of broadly distributed resistor networks. *Physica B*, *338*(1-4), 266–269. https://doi.org/10.1016/j.physb.2003.08.005
Skaggs, T. H. (2011). Assessment of critical path analyses of the relationship between permeability and electrical conductivity of pore networks. *Advances in Water Resources*, *34*(10), 1335–1342. https://doi.org/10.1016/j.advwatres.2011.06.010
Sněhota, M., Císlerová, M., Amin, M. H. G., & Hall, L. D. (2010). Tracing the entrapped air in heterogeneous soil by means of magnetic resonance imaging. *Vadose Zone Journal*, *9*(2), 373–384. https://doi.org/10.2136/vzj2009.0103
Stauffer, D., & Aharony, A. (1994). *Introduction to percolation theory* (2nd ed.). London: Taylor and Francis.
Tsai, D.-M. (1995). A fast thresholding selection procedure for multimodal and unimodal histograms. *Pattern Recognition Letters*, *16*(6), 653–666. https://doi.org/10.1016/0167-8655(95)80011-H
Udawatta, R. P., Anderson, S. H., Gantzer, C. J., & Garrett, H. E. (2008). Influence of prairie restoration on CT-measured soil pore characteristics. *Journal of Environmental Quality*, *37*(1), 219–228. https://doi.org/10.2134/jeq2007.0227
Vereecken, H., Weynants, M., Javaux, M., Pachepsky, Y., Schaap, M. G., & van Genuchten, M. T. (2010). Using pedotransfer functions to estimate the van Genuchten-Mualem soil hydraulic properties: A review. *Vadose Zone Journal*, *9*(4), 795–820. https://doi.org/10.2136/vzj2010.0045
Wösten, J. H. M., Pachepsky, Y. A., & Rawls, W. J. (2001). Pedotransfer functions: Bridging the gap between available basic soil data and missing soil hydraulic characteristics. *Journal of Hydrology*, *251*(3-4), 123–150. https://doi.org/10.1016/S0022-1694(01)00464-4